Parametric structure optimization of a main rotor blade as an application for FSI analysis in main rotor optimization process

Jakub Kocjan
Doctoral School, Military University of Technology, Warsaw, Poland, and

Robert Rogólski
Faculty of Mechatronics, Armament and Aerospace, Military University of Technology, Warsaw, Poland

Abstract

Purpose – Modern warfare and modern battlefield are very demanding. The recent conflicts showed that the usage of the helicopters is very limited and only the best constructions are able to provide support for the operations. The purpose of this research is to show the possibilities of new design tool for main rotor aerostructural optimization. It is a next chapter of the research that is aimed at finding new solutions for rotorcraft constructions.

Design/methodology/approach – This work presents a method of preliminary structure optimization of the main rotor blade using parametric modeling. It is the next step in the main rotor optimization studies. It is the next step after preparing the parametric model for the external shape CFD analysis. As a basis for parametric blade structure calculations, the analytical model is provided in this paper. The equations of rigid blade loads and, as a consequence of the strength elements, stresses are shown. The parametric blade modeling is conducted using the Graphic Integrated Programming language. The parametric design method is shown to be used for various blade planform models and different section airfoils. The structure of a blade is generated automatically after the user enters the parameters. The code-inbuilt analysis systems provide a quick inertia examination of the generated geometry, which is the basis for further optimization. The program calculates the blade loads and verifies them with the given material conditions and proposed safety factors. In the analysis, composite materials for the strength elements were proposed.

Findings – The results of this research showed the application of parametrization into the main rotor blade design loop. It was presented that the main rotor blade structure can be enhanced using fluid-structure interaction (FSI) methods. The time saving with the implementation the process into design loop is shown.

Practical implications – This work can be practically used in the main rotor blade design process. It provides the possibilities to check various blade aerodynamic configuration in a structure strength aspect.

Originality/value – To the best of the authors' knowledge, there were no published research that combines the main rotor FSI analysis. The method, which is presented in the work, provides a new approach to a rotorcraft design. The application of the parametrization and combining it with the FSI method gives a novel solution for helicopters construction enhancement.

Keywords Helicopter, Rotorcraft, Optimization, Main rotor, Fluid-structure interaction

Paper type Research paper

Introduction

The recent military conflicts have prompted a reassessment of the possible operations that helicopters can conduct on the modern battlefield. The need for constructions capable of providing enhanced characteristics for widespread military operations has been acknowledged by manufacturers and national authorities. Consequently, many countries are upgrading current configurations and exploring new solutions for vertical take-off and landing vehicles. Therefore, at the Military University of Technology, studies focused on finding new approaches and design possibilities for rotorcraft are

The current issue and full text archive of this journal is available on Emerald Insight at: **https://www.emerald.com/insight/1748-8842.htm**

Aircraft Engineering and Aerospace Technology
97/1 (2025) 37–51
Emerald Publishing Limited [ISSN 1748-8842]
[DOI 10.1108/AEAT-03-2024-0084]

This work was financed by the Military University of Technology (Warsaw, PL) under the two following research projects: No. UGB 22-732/2024/WAT entitled: Aerodynamic design of aircraft in terms of optimizing selected performance parameters; No. UGB 22-734/2024/WAT entitled: Design of light aircraft lifting structures in terms of optimizing strength and aeroelastic properties of the airframe. Both grants were carried out in the Institute of Aviation Technology (Faculty of Mechatronics, Armament and Aerospace of the Military University of Technology) in the year 2024 as university statutory activities funded by the Ministry of National Defence of the Republic of Poland.

Received 29 March 2024
Revised 12 July 2024
Accepted 5 September 2024

underway. The research began with an evaluation of helicopter construction features and parameters responsible for rotorcraft performance. The analysis considered nearly 70 of the newest helicopter designs from around the world. The results of this comparison were published in Kachel *et al.* (2021).

The main goal of the entire research is to develop a multicriteria optimization procedure to provide a solution using the newest computer-aided design methods. There are several main approaches to resolving optimization problems nowadays. The results of research focused on main rotor aerodynamic optimization are published in Okumuş *et al.* (2022), Stalewski (2017), Stalewski and Zalewski (2019), Tamer *et al.* (2011) and Xie *et al.* (2017), whereas an example addressing strength problems is shown in Spyropoulos *et al.* (2021). Some research institutes concentrate on main rotor optimization problems, such as the ONERA French Aerospace Lab and the DLR German Aerospace Centre. Their results are presented in Goerke *et al.* (2012), Pahlke and Demaret (2017), Tremolet and Basset (2012) and Wilke (2021, 2024). The proposed solution involves using parametrization in CAD geometry design. The benefits of using this approach were presented in Sagimbayev *et al.* (2021) and MA *et al.* (2021). Parametrization is also currently used for airfoil design (Allen *et al.*, 2021; Lim, 2018; Vu and Lee, 2015), structural design (Tixadou, 2021; Гребеников *et al.*, 2021) and aerodynamic design (Bailly *et al.*, 2019). Therefore, the second step, following comparative analysis, was the preparation of the main rotor blade shape as a parametric model using the Graphic Integrated Programming (GRIP) language. The evaluation of the model's application in CFD analysis was published in Kocjan *et al.* (2022). In addition, in further research, the CFD fluid domains were parametrized and simultaneously generated with a full n-bladed rotor for CFD analysis under different flight conditions. The aim of preparing the CFD environment and parametrizing the rotor model and its enclosures is to obtain a solution for quick preparation of (fluid-structure interaction) analysis.

The second part of preparing the FSI analysis involves setting up a finite element structural loads simulation. Therefore, to integrate it with the optimization procedure, a parametric structural model also needs to be prepared. This paper presents the preparation of a model for further analysis with preliminary strength analytical calculations. The preparation of the CAD parametric model is conducted using the GRIP language, which is implemented in Siemens NX software. Examples of GRIP usage are shown in Grabowik *et al.* (2015), Ryazanov (2016) and Shabliy and Dmitrieva (2014). This language provides the capability to generate external body or inner structural parts of the airframe that are currently being designed. Within the code, mathematical calculations, logical conditions and geometry creation are possible. The main advantages of the presented solution, which will be demonstrated in this research, include mass and inertia analysis built within the code. The functions offer the possibility to obtain numerical features of any geometry shapes, which can be used to prepare an optimization procedure. The program code presented in this paper, which generates geometry preliminarily prepared and calculated for given flight conditions, is prepared by the authors.

Another approach to main rotor blade optimization is the aeroelastic features optimization. Researches that are conducted nowadays are focused on enhancing features that concerns also the vibration of the blade. One of the most interesting studies are the influence of the BERP-like blade tip on working conditions and aeroelastic response (Johnson *et al.*, 2016; Moffatt and Griffiths, 2009). In this kind of studies also the computer methods are used. Some examples of the CFD analysis including vibrations analysis are shown in Allen *et al.* (2009) and Cornette *et al.* (2015). However, the exploration that are aimed at single or multicriteria optimization, that takes into account the main rotor blades aeroelastic attributes, are valuable and shows the procedures to obtain the best main rotor attributes. This is also the aim of research described in this paper. Very good examples of the optimization mentioned above are (Ganguli and Chopra, 1996; Guo and Xiang, 2004; Kizhakke Kodakkattu *et al.*, 2018; Liu and Zhang, 2021; Morris *et al.*, 2008; Straub *et al.*, 1992; Tarzanin *et al.*, 1999; Wang *et al.*, 2013). As it can be spotted there is many research that provides the solution for optimization and vibration reduction; however, there is not many published papers that use the FSI method for that purpose. One example is presented in Sinem and Metin Orhan (2018).

The optimization of the blade structure is described in Barwey and Peters (1994), Chattopadhyay *et al.* (1995), He and Peters (1992), Tian *et al.* (2022), and Vu *et al.* (2016) in which various aspects of the structure are taken into consideration. The most significant for the presented research are the strength considerations in aspects of its aerodynamic loads; however, the proposed procedures have not been developed using modern computational techniques. The example of modern optimization research where the advanced analysis is presented was published in Salh Eddine *et al.* (2023).

Taking into consideration the conducted analysis of research that were performed in helicopter main rotor design enhanced with optimization techniques, there is lack of the studies that combine the parametrization of the rotor blade for both numerical and analytical analysis, where the analytical model takes into consideration the inertia and mass features of the structure.

The novelty of this study lies in combining analytical research with computer analysis of the blade structure to obtain exact mass and inertia parameters and optimize the shape of the spar across various spar cross-sections.

The analytical analysis for generating the structure is conducted using MATLAB software. Originally developed codes, with implemented mathematical formulas, calculate main rotor loads and bending moments. The generated loads are presented graphically as functions of radius and azimuth. The natural frequencies are also shown in charts. The process of generating the load and frequency shapes is automated and implemented into the code. The program recalculates the inertia parameters at selected cross sections of the blade, providing a comprehensive tool for analyzing structural features and working conditions. Consequently, the designer can quickly evaluate the case and identify possible weak points and faults.

Calculated loads are transferred into a CAD parametric optimization program (prepared using GRIP), where the shape is formed and assessed to meet the given material properties using an optimization procedure. The research also introduces features of modern composite structures.

To the best of the authors' knowledge, the approach presented in this paper has not been combined in any known research, making it unique in main rotor blade structure design studies.

Analytical model

Main rotor aerodynamic load

To estimate the main rotor aerodynamic loads for structural analysis, it is necessary to calculate the main rotor trim angles. The method of trimming was described in the previous phase of the study (Kocjan *et al.*, 2022) Trimming can be performed for all types of flight conditions. Finding pitch angles and flap angles is the first step in determining the main rotor blade load:

$$\theta(\psi) = \theta_0 - \theta_1\cos(\psi) - \theta_2\sin(\psi) \tag{1}$$

$$\beta(\psi) = \beta_0 - \beta_1\cos(\psi) - \beta_2\sin(\psi) \tag{2}$$

where θ are pith angles, β are flap angles and the ψ is rotor blade azimuth. The rotor motion is shown in Figure 1.

The rotor thrust which can be assumed as a rotor lift is given with the equation:

$$dT = \frac{1}{2}a\rho\left(\theta U_T^2 + U_p/U_{UT}\right)dr \tag{3}$$

where a is the lift curve slope and ρ is the air density. However, to calculate the thrust an velocity components at the blade are needed to be estimated:

$$U_p = \Omega\mathrm{R}\left(\lambda' - \frac{x\dot{\beta}}{\Omega} - \mu\beta\cos\psi\right) \tag{4}$$

$$U_T = \Omega\mathrm{R}(\mathrm{x} + \mu\sin\psi) \tag{5}$$

where Ω is main rotor rotational velocity, R is the rotor radius, and μ is the advance ratio. The inflow ratio is given with:

$$\left(\lambda' = (V\sin\alpha_D - \nu_i)/\Omega\mathrm{R}\right. \tag{6}$$

where V is the rotorcraft velocity α_D is rotor disc angle of attack and ν_i is the rotor induced velocity.

Rotor blade normal modes and frequencies

Estimating the bending shapes of the rotor blade requires calculating the natural frequencies and normal modes. There is no single technique or procedure to determine the values of vibration parameters. For this research, the Rayleigh–Ritz method was chosen, and the algorithm used is based on (Wilde and Price, 1965) In this method, the energy equation of the rotating beam is minimized:

$$\epsilon = \int_0^R \left\{EI\left(\frac{d^2y}{dr^2}\right)^2 + \frac{1}{2}\overline{m}\Omega^2(R^2 - r^2)\left(\frac{dy}{dr}\right)^2 - m\omega^2y^2\right\}dr \tag{7}$$

where E is the Young Modulus, I is the second moment of area, y is the natural mode shape and ω is the natural frequency.

The applied method of solution provides possibilities for using the method in numerical software. The equation is transformed into matrix form, with each part being transformed into Fourier series. This allows for the application of nonconstant mass distribution into the procedure and enables the utilization of the orthonormality properties of Fourier series. To further simplify the procedure, the spanwise coordinate is given as $x = \pi r/R$. Then the equation's components are:

$$\frac{EI(x)\pi^2}{R} = \sum_1^\infty p_n\cos nx \tag{8}$$

$$\frac{\overline{m}\Omega^2R^2(\pi^2 - x^2)}{2\pi^2} = \sum_1^\infty q_n\cos nx \tag{9}$$

$$y = a_0x - \sum_1^\infty a_n\sin nx \tag{10}$$

Substituting the parts of energy expression we get:

$$E = \int_0^\pi\left\{\left(\sum_1^\infty p_n\cos nx\right)\left(\sum_1^\infty n^2a_n\sin nx\right)^2 + \left(\sum_1^\infty q_n\cos nx\right)\left(a_0 - \sum_1^\infty na_n\sin nx\right)^2 - r_0\omega^2\left(a_0x - \sum_1^\infty a_n\sin nx\right)^2\right\}dx \tag{11}$$

These equation can be written in a matrix form and A and B are symmetric matrices with p and q coefficients:

$$\left(A^{-1}B - \frac{I}{\Gamma^2}\right)\underline{a} = 0 \tag{12}$$

where $\Gamma^2 = 2\omega^2r_0$ and a is the matrix of coefficients of normal modes shape. Calculating the latent roots of the matrix $A^{-1}B$ the natural frequencies and shapes are obtained.

Rotor flapping blade bending moment

After preparing the earlier results, the bending moment can be estimated for different spanwise coordinates and azimuthal locations. The first step is to establish the external forces on the blade. These external forces consist of:

- the elementary lift $dT=dF_a$;
- the blade weight $m'gdx$;
- centrifugal force of rotation $m'\omega^2r\beta dx$;
- the force inertia for flapping $-mx\ddot{\beta}$;
- the force of inertia of deflection $-mx\ddot{y}$;
- the centrifugal force of flapping $m'x\dot{\beta}2$;

Figure 1 Rotor velocity and blade motion

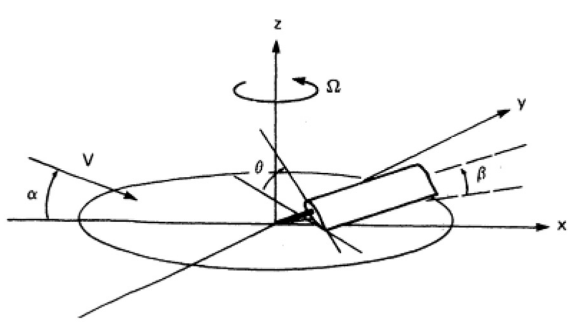

Source: Reproduced from Johnson (1994)

- the Coriolis force due to the simultaneous action of blade deflection and flapping motion $-2\dot{\beta}\dot{y}m'$; and
- corrective term of the damping of the lift force due to the flexural elastic deformation of the blade $-K\dot{y}$.

In this calculation, the Euler–Bernoulli beam theory was chosen. In this theory, the main assumptions are that the cross section of the beam is rigid (i.e. no deformations occur in the plane of the cross section), and shear deformations are neglected. The cross section remains plane, unstretched and normal to the deformed axis of the beam after deformation.

Authors resigned from using the Timoshenko beam theory, which is mostly used in the case of short or thick beams where shear effects can be significant. This theory includes the effects of shear deformation. As a result, the difference in Timoshenko theory is that after deformation, the cross section of the beam is no longer normal to the beam axis. As mentioned above, this effect can be neglected.

The differential equation of the blade is then:

$$\frac{d^2}{dx^2}\left(EI\frac{d^2y}{dx^2}\right)-\omega^2\frac{d}{dx}\left(\frac{dy}{dx}\int_x^R m'(a+\xi)d\xi\right)+m^{'\ddot{y}}+K\dot{y} = \frac{dF}{dx}-m'g-mx\ddot{\beta}-m'\omega^2 r\beta \tag{13}$$

The differential equation must be fulfilled by four conditions, which specify the integration constants:

$$y=0 \ \text{ for } x=0 \tag{14}$$

$$EI\frac{d^2y}{dx^2}=0 \text{ for } x=0 \text{ and for } x=R-a \tag{15}$$

$$\frac{d^2}{dx^2}\left(EI\frac{d^2y}{dx^2}\right)=0 \text{ for } x=R-a \tag{16}$$

To solve the deflection equation the second member, which is independent of the deflection can be put into function $dF_d = \mathrm{dFa} - \ m'g - \ m'\omega 2\ x - mx\,\ddot{\beta}$. We also put: $\int_x^R m'(a+\xi)d\xi = S$ so the final form is:

$$\frac{d^2}{dx^2}\left(EI\frac{d^2y}{dx^2}\right)-\omega^2\frac{d}{dx}\left(s\frac{dy}{dx}\right)+m'\ddot{y}+K\dot{y}=\dot{F}_d'(x,t) \tag{17}$$

The applied calculation formula estimates the distribution of bending moment to the third harmonic of natural shape. This method was chosen due to its compatibility with the MATLAB environment.

Initially, we use the natural deflection functions of the rotor blade to solve it. For simplicity, we consider the vibration state to be undamped. The bending moment is assumed to result from the forces acting on the rigid blade. In addition, the time function can be expanded into a series of periodic functions, represented as $\psi=\omega t$, therefore:

$$M_{rig}=M_0+M_a\cos\psi+M_b\sin\psi+M_{2a}\cos2\psi+M_{2b}\sin2\psi + M_{3a}\cos3\psi+M_{3b}\sin3\psi\ldots \tag{18}$$

This moment concerns the distribution of external force F_d' which constitute the second term of the equation. These forces should also be resolved at each point as a series of deflection distributions correlated with the natural mode shape. The natural functions can always be resolved into series. The proposed series take form:

$$F_d' = g_0 m'\eta_0 + g_1 m'\eta_1 + g_2 m'\eta_2 + \ \ldots \tag{19}$$

where g_i is the function a function of time only and η_i is the bending natural function of the order i.

The i order deflection of the main rotor blade affects at each point the natural mode function, it is given by function:

$$y_i = h_i\eta_i \tag{20}$$

where h_i is the function of time. The deflection is obtained by superposing the many natural deflections of the blade vibrating at the corresponding natural frequencies, using the h_i function which defines the amplitude and phase. Therefore, for the i-order frequency:

$$h_i\frac{d^2}{dx^2}\left(EI\frac{d^2\eta_i}{dx^2}\right)-h_i\omega^2\frac{d}{dx}\left(s\frac{d\eta_i}{dx}\right)+h_i m^{'\ddot{y}} = g_i m'\eta_i \tag{21}$$

Next, the natural vibrations of a freely vibrating blade with an angular velocity ω allow an infinite quantity of solutions, using η *sinvt* a function a limiting conditions and the below function is satisfied:

$$\frac{d^2}{dx^2}\left(EI\frac{d^2\eta}{dx^2}\right)-\omega^2\frac{d}{dx}\left(s\frac{d\eta}{dx}\right)=\nu^2 m'\eta_i \tag{22}$$

As a consequence, for the natural function we obtain a rotating beam function for every natural frequency:

$$\frac{d^2}{dx^2}\left(EI\frac{d^2\eta_i}{dx^2}\right)-\omega^2\frac{d}{dx}\left(s\frac{d\eta_i}{dx}\right)=\nu_{i,\omega}^2 m'\eta_i \tag{23}$$

where $\nu_{i,\omega}$ is the corresponding function of natural frequency at the ω speed of rotation.

When the equations are simplified, the result is:

$$h_i\nu_{i,\omega}^2+\ddot{h}_i=g_i \tag{24}$$

The functions given above $h_i\, g_i$ are periodic with respect to ψ, so there can be transformed into series:

$$h_i = h_{i,0}+h_{i,a}\cos\psi+h_{i,b}\sin\psi+h_{i,2a}\cos2\psi+h_{i,2b}\sin2\psi + h_{i,3a}\cos3\psi+h_{i,3b}\sin3\psi\ldots \tag{25}$$

$$g_i = g_{i,0}+g_{i,a}\cos\psi+g_{i,b}\sin\psi+g_{i,2a}\cos2\psi+g_{i,2b}\sin2\psi + g_{i,3a}\cos3\psi+g_{i,3b}\sin3\psi\ldots \tag{26}$$

Therefore, the differential equation can be written:

$$\sum_{i=0}^{i=\infty}\left[h_i\frac{d^2}{dx^2}\left(EI\frac{d^2\eta_i}{dx^2}\right)-h_i\omega^2\frac{d}{dx}\left(s\frac{d\eta_i}{dx}\right)+h_i m'\ddot{y}\right] = \sum\nolimits_{i=0}^{i=\infty} g_i m'\eta_i \tag{27}$$

Limiting the equation to third harmonic and resolving the identification of the coefficients, it can be reduced into:

$$h_{i,0}\nu_{i,\omega}^2 = g_{i,0} \tag{28}$$

$$h_{i,a}\left(\nu_{i,\omega}^2 - \omega^2\right) = g_{i,a} \tag{29}$$

$$h_{i,b}\left(\nu_{i,\omega}^2 - \omega^2\right) = g_{i,b} \tag{30}$$

$$h_{i,2a}\left(\nu_{i,\omega}^2 - 4\omega^2\right) = g_{i,2a} \tag{31}$$

$$h_{i,2b}\left(\nu_{i,\omega}^2 - 4\omega^2\right) = g_{i2b} \tag{32}$$

$$h_{i,3a}\left(\nu_{i,\omega}^2 - 9\omega^2\right) = g_{i,3a} \tag{33}$$

$$h_{i,3b}\left(\nu_{i,\omega}^2 - 9\omega^2\right) = g_{i3b} \tag{34}$$

To determine the g_i it is needed to multiply the members of the equation (19) by η_i and conduct integration over the blade.

Taking into consideration the orthogonality condition:

$$\int_0^R m'\eta_i\eta_j dx = 0 \qquad i \neq j \tag{35}$$

it provides:

$$\int_0^R F'_d\eta_i dx = g_i\int_0^R m'\eta_i{}^2 dx \tag{36}$$

$$g_i = \frac{\int_0^R F'_d\eta_i dx}{\int_0^R m'\eta_i{}^2 dx} \tag{37}$$

Next, the bending moment on the deformable main rotor blade is computed. The single harmonic acting the outside forces, produces the elastic deformation:

$$\sum_{i=1}^{i=\infty}\left[g_{i,na}m'\eta_i\cos n\psi + g_{i,nb}m'\eta_i\sin n\psi\right] \tag{38}$$

which is:

$$\sum_{i=1}^{i=\infty} y_{i,n}\begin{Bmatrix} a \\ b \end{Bmatrix} = \sum_{i=1}^{i=\infty} h_{i,n}\begin{Bmatrix} a \\ b \end{Bmatrix}\eta_i \tag{39}$$

When the terms h_i are replaced by values which are obtained from (28–34), the corresponding bending moment:

$$M_{elast\ n}\begin{Bmatrix} a \\ b \end{Bmatrix} = \frac{g_{i,n}\begin{Bmatrix} a \\ b \end{Bmatrix}}{\nu_{i,\omega}^2 - n^2\omega^2} - EI\frac{d^2\eta_i}{dx^2}\begin{Bmatrix} \cos n\psi \\ \sin n\psi \end{Bmatrix} \tag{40}$$

Because the natural functions exhibit minimal variation with changes in angular velocity, the ith order natural function at $\omega = 0$, is comparable to the same natural function for the standard angular velocity. This simplification incurs an error of only 3%, making it suitable for application in this solution.

As a consequence, the natural function η_i fulfills the equation (23) and:

$$\frac{d^2}{dx^2}\left(EI\frac{d^2\eta_i}{dx^2}\right) = \nu_{i,0}^2 m'\eta_i \tag{41}$$

In result:

$$EI\frac{d^2\eta_i}{dx^2} = \nu_{i,0}^2\iint_x^R m'\eta_i dx d\xi \tag{42}$$

After replacing in (40) the value of $EI\frac{d^2\eta_i}{dx^2}$ with (42), the elastic blade bending moment equation is obtained, which is can be integrated along the blade:

$$M_{elast\ n}\begin{Bmatrix} a \\ b \end{Bmatrix} = \sum_{i=1}^{i=\infty}\left(\frac{\nu_{i,0}^2}{\nu_{i,\omega}^2 - n^2\omega^2}g_{i,n}\begin{Bmatrix} a \\ b \end{Bmatrix}\iint_x^R m'\eta_i dx d\xi\right) \tag{43}$$

The value of the g_i is calculated from (37) for the azimuth values for a given acting forces. The expansion of the g_i into Fourier series expresses the coefficient:

$$g_{i,n}\begin{Bmatrix} a \\ b \end{Bmatrix} \tag{44}$$

Practical bending moment calculation procedure

Considering the equation calculation, a practical calculation method is proposed in de Guillenchmidt (1951). This method offers a step-by-step solution that can be applied to numerical calculations. The first step, as described earlier, involves calculating the natural functions and corresponding natural frequencies of both rotating and nonrotating blades. In the second step, we evaluate the values:

$$\int_0^R m'\eta_1{}^2 dx\int_0^R m'\eta_2{}^2 dx\int_0^R m'\eta_3{}^2 dx \tag{45}$$

Next step is to determine the outside forces on the rigid main rotor blade for different ψ (minimum eight positions with 45° spacing), so the position are evaluated for:

$$\int_0^R F'_d\eta_1 dx\int_0^R F'_d\eta_2 dx\int_0^R F'_d\eta_3 dx \tag{46}$$

Taking into consideration the (37) equation the function are calculated:

$$g_1 = \frac{\int_0^R F'_d\eta_1 dx}{\int_0^R m'\eta_1{}^2 dx}\; g_2 = \frac{\int_0^R F'_d\eta_2 dx}{\int_0^R m'\eta_2{}^2 dx}\; g_3 = \frac{\int_0^R F'_d\eta_3 dx}{\int_0^R m'\eta_3{}^2 dx} \tag{47}$$

The function (47) can be developed into Fourier series. The series are produced to third harmonic of ψ:

$$\begin{matrix} g_{1,0} & g_{1,a} & g_{1,b} & \cdots & g_{1,3b} \\ g_{2,0} & g_{2,a} & g_{2,b} & \cdots & g_{2,3b} \\ g_{3,0} & g_{3,a} & g_{3,b} & \cdots & g_{3,3b} \end{matrix} \tag{48}$$

The bending moments are calculated for each harmonic and for different station on the blade span using equation:

$$M_x = \sum_{i=1}^{i=3} M_{i,x} \tag{49}$$

The inner functions are estimated with:

$$\begin{aligned} M_{i,x} = \iint_x^R m' \eta_i dx d\xi \big[A_{i,0} + A_{i,1}\cos(\psi - \psi_{i,1} - \varphi_{i,1}) \\ + A_{i,2}\cos(2\psi - \psi_{i,2} - \varphi_{i,2}) \\ + A_{i,3}\cos(3\psi - \psi_{i,3} - \varphi_{i,3}) \big] \end{aligned} \tag{50}$$

where

$$A_{i,0} = \frac{\nu_{i,0}^2}{\nu_{i,\omega}^2} g_{i,0} \tag{51}$$

$$A_{i,n} = \frac{\nu_{i,0}^2 \sqrt{g^2{}_{i,na} + g^2{}_{i,nb}}}{\sqrt{\left(\nu_{i,\omega}^2 - n^2\omega^2\right)^2 + n^2\Phi^2\omega^4}} \tag{52}$$

$$\tan\psi_{i,n} = \frac{\omega^2 n \Phi}{\left(\nu_{i,\omega}^2 - n^2\omega^2\right)} \tag{53}$$

$$\tan\varphi_{i,n} = \frac{g_{i,nb}}{g_{i,na}} \tag{54}$$

Optimization method

As it was mentioned in introduction this paper presents the part of research that is aimed at finding solutions for main rotor optimization problem. The proposed algorithm for the entire program is presented on Figure 2. The structure optimization is an inner procedure inside the presented loop. It is included inside the "parametric modelling" element, where the outer shape and CFD enclosures are generated, as well as the blade inner structure.

The inner structure optimization is performed using computer techniques; however, some mathematical assumptions must be made. This procedure is a single-criterion mass reduction process while maintaining the required strength. The mathematical description is presented below:

- *Decision variables*: h – spar height, d – honeycomb wall position, t – spar thickness
- *Parameters*: material properties, flight conditions
- *Constraints*: σdop > σmax(h, d, t) – strength condition; $h > 0$, $t > 0$, max airfoil thickness position > d >0
- *Criteria*: $m(h, d, t) \rightarrow$ minimum

The process of resolving main rotor blade stresses and subsequently optimizing the shape is divided into steps, with each step described in consecutive chapters.

The first phase of the proposed method involves resolving the mathematical model presented in Chapter 2. This model was implemented in the MATLAB environment to solve equations and compute values for rotor parameters. The results serve as the basis for a customized GRIP program to assess the best structural shape.

Figure 2 Main rotor optimization research algorithm

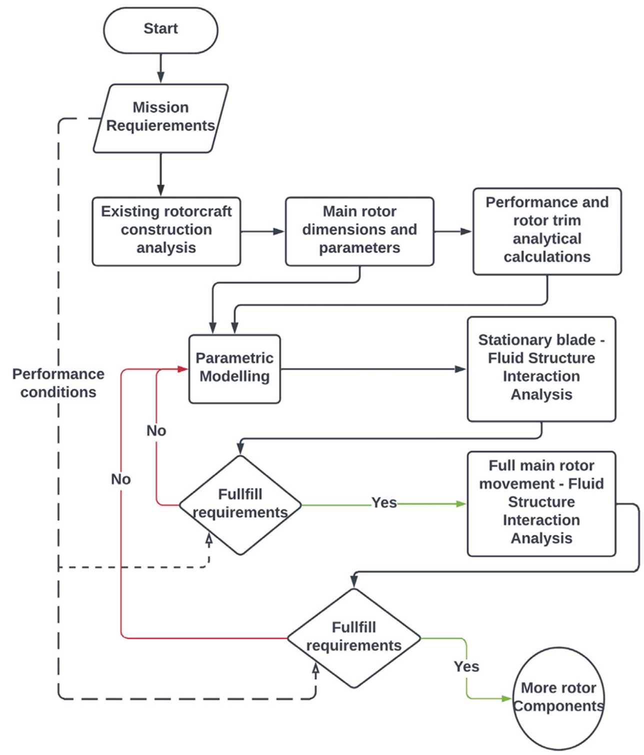

Analytical solving

The problem was divided into two separate codes. The first one was prepared for the main rotor trim, involving calculations of blade loads. The second one focused on blade mode shapes, natural frequencies, and finally, the determination of bending moment values and distribution.

To initiate the calculations, the first code begins with declaring the geometric and aerodynamic parameters of the main rotor. Basic helicopter parameters, especially weight, are also included. In the input section, initial blade mass parameters are declared. These parameters can be based on an existing blade or estimated using statistical data from similar constructions. Such statistics were compiled in the initial phase of the research program (Kachel *et al.*, 2021).

In addition, the user declares the flight conditions under which the main rotor blade stresses are evaluated. These conditions describe the flight with the forward speed and climb, and include the statistical change of the center of gravity as a function of velocity. The forward speed is also calculated in the form of an advance ratio.

The next step involves parameterizing the rotor chord and twist so that their values can vary along the span. The calculated coefficients will also be used in the program that generates the geometry for structural evaluation.

The subsequent stage of the procedure involves trimming the main rotor pitch and flap angles. The code has been partially prepared in previous phases of the research. Trim angles are determined by resolving acting forces horizontally and vertically with reference to the rotor-disc plane. After acquiring the trim angles, the blade aerodynamic loading can be determined. By solving the equations of velocity components, the lift distribution is obtained. Examples of aerodynamic loading distribution generated using the MATLAB environment are shown in Figure 3, whereas the total aerodynamic loading is depicted in Figure 4. These figures illustrate that the calculated loading offers a means to evaluate the rotor's working conditions. It can be seen that the behavior of aerodynamic forces slightly changes with inflow ratio increase. Especially on advancing blade position (azimuth 135° represents the transition position), where the influence of maximum forward speed, due to the inflow angle change, is reducing the aerodynamic force. The blade geometric twist is provided to reduce the diminish the negative force value.

The second calculation program, which receives the aerodynamic loading from the first procedure, is used to find first the natural modes and frequencies and next solve the bending moment equation. It also includes the declaration of inputs part of the code, where the geometry and mass dimensions of the rotor are given. In this phase, the stiffness declaration is provided as a function of material Young modulus and moment of inertia. The stiffness alters along the span due to the change of cross section of the blade spar. The moments of inertia are established using the GRIP program, which will be described later.

Furthermore, the program calculates the natural mode shapes and frequencies. The calculation procedure implemented in the code is described in section Rotor blade normal modes and frequencies. Matrices are prepared to compute the vibration quantities up to the 8th harmonic. Using the built-in functions of MATLAB, the results are easily obtained. Functions are transformed into Fourier series using the Fourier Series integral definition, and then matrices of coefficients are constructed. The eigenvalues of the matrices equation are determined using MATLAB's built-in functions. The characteristics can be evaluated for every shape of a blade and materials that are used. Exemplary results for the rotor blade (W-3 helicopter rotor blade shape) are depicted in Figure 5. The natural function value is normalized and the radius is parameterized as a function of π.

Figure 3 Aerodynamic loading distribution for different inflow ratio (flight speed)

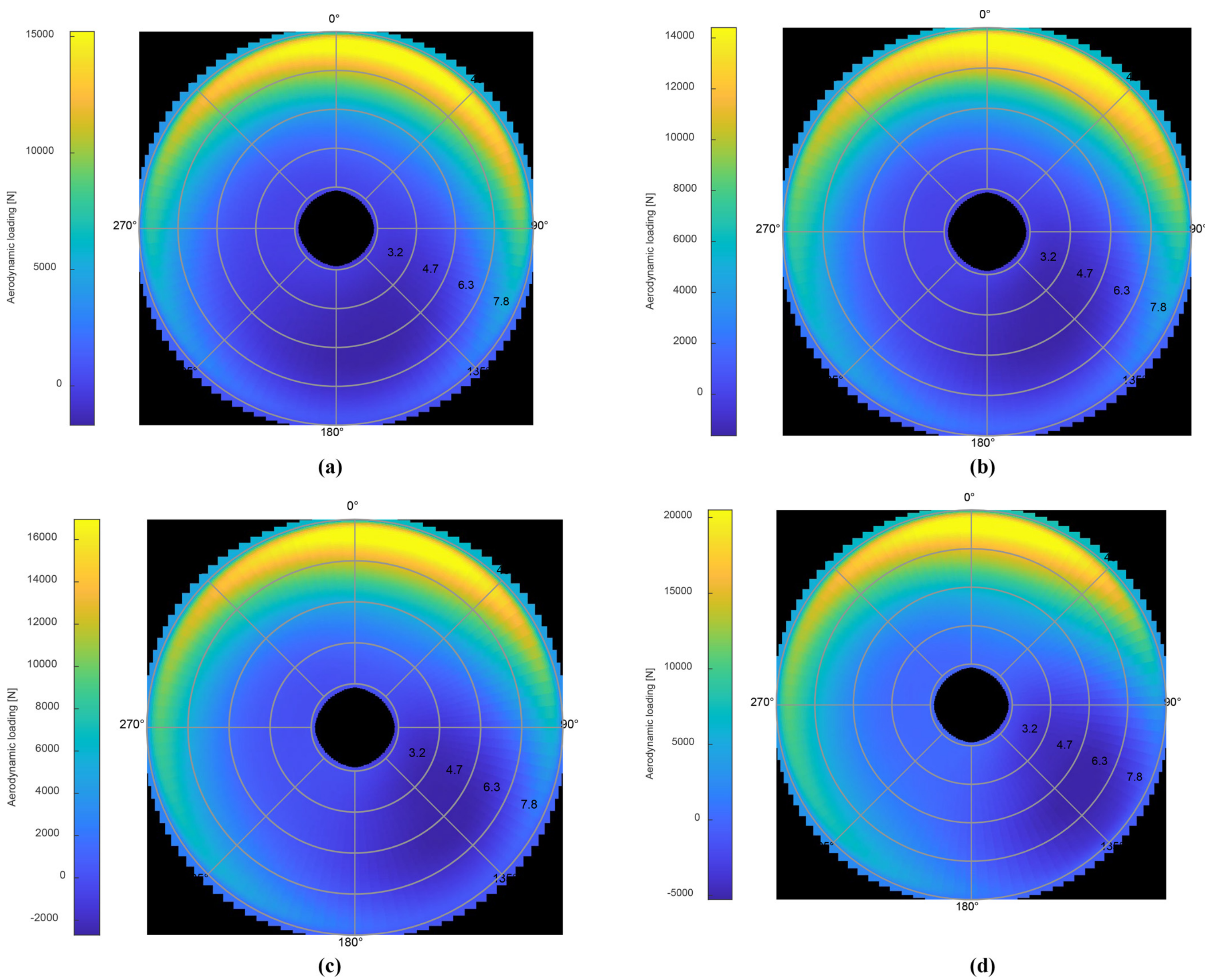

Note: (a) $\mu = 0.1$; (b) $\mu = 0.15$; (c) $\mu = 0.2$; (d) $\mu = 0.25$

Figure 4 Aerodynamic loading in function of radius for: $\mu = 0.1$

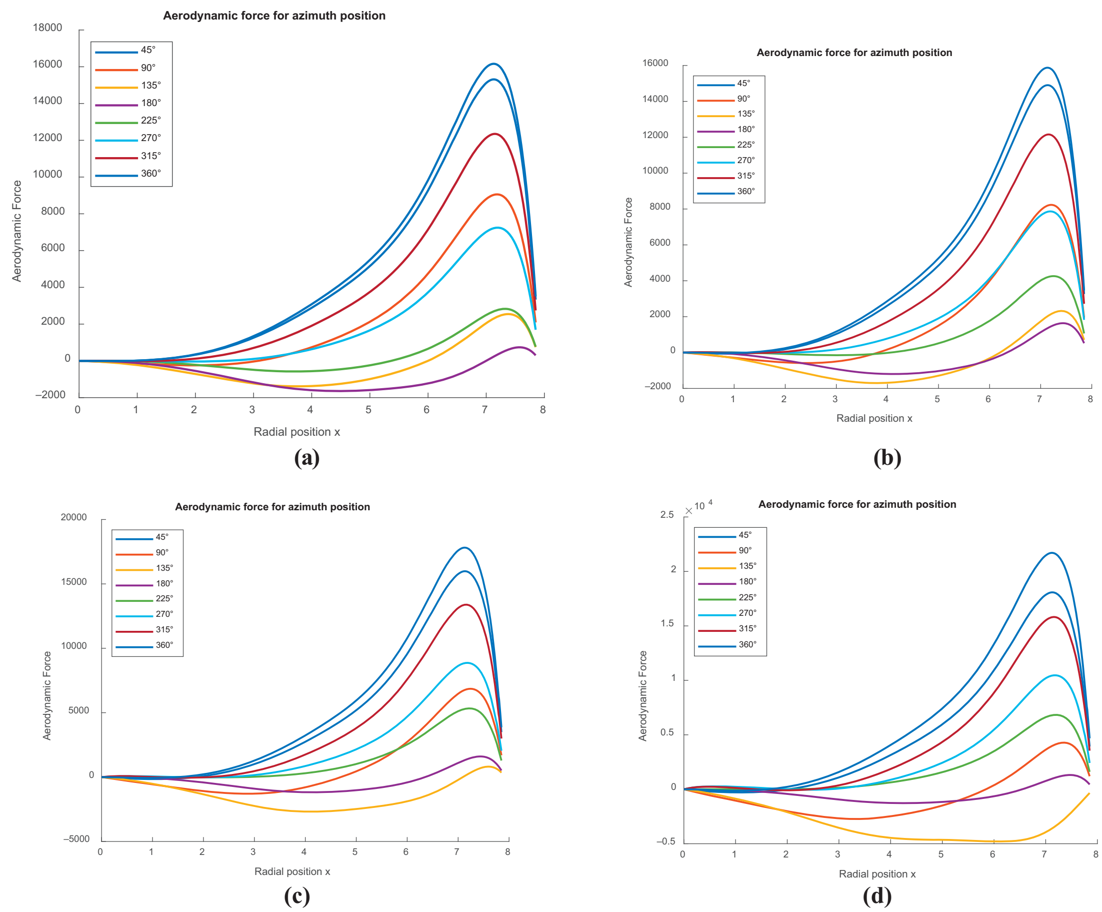

Note: (a) $\mu = 0.1$; (b) $\mu = 0.15$; (c) $\mu = 0.2$; (d) $\mu = 0.25$

In the next step of the code execution, the bending moment for the first three harmonics is obtained. The outside forces, established in the first program and described in section Main rotor aerodynamic load, are input for the aerodynamic loading. The damping coefficient is estimated, and then the outside force and mass distribution are correlated with the natural vibration shape. The procedure is applied as follows: the time functions g_i are calculated for each harmonic, and the resultant equations are substituted into the bending moment function, respectively, to the harmonic number. The calculations end with summing the total bending moment, which is a function of radius and azimuth. An example of the values of bending moment depending on the radius and azimuth is shown in Figure 6. The maximum bending moment values are written into a file to serve as input for geometry strength analysis.

Graphics integrated programming

The primary objective of this study is to develop a new method for preparing the main rotor blade geometry for FSI analysis and optimization. The aim is to reduce the time consumption of complex simulations and find the best strength structure by combining analytical calculations with the capabilities of open GRIP inertia analysis code, which is an integral part of Siemens NX. The program has been partially used because the initial stages of the study, as the external geometry needs to be exact for further FSI simulations, ensuring connections of corresponding faces.

The blade model is parametrized in the program using main rotor geometric features. The designer can input values into a popup input window, corresponding with the input values from MATLAB programs. The first parameter is the blade chord and rotor radius. The airfoil is shaped from a text file with the coordinates, allowing the operator to prepare the geometry for any chosen airfoil. The next phase of parametrization involves polynomial coefficients for twist and chord of the blade, allowing them to vary along the span. The outer model is filled with the structure. The inner assembly of the blade is based on existing solutions, with the main spar and filling in the leading edge part, and a honeycomb structure in the trailing edge part. An illustration of the CAD model is shown in Figure 7.

With the prepared solution, the blade shape can be freely changed in accordance with the analytically calculated values. The shape building process relies on built-in GRIP commands for lines and splines, which are used to create the requested shape.

Furthermore, the program conducts the analysis and strength calculation. Using integral commands, the mass and inertia analysis of the cross sections and the entire 3D geometry are performed. As a result, the moment of inertia of cross sections is obtained. The density of the parts is programmed by the user,

Figure 5 Natural modes and frequencies

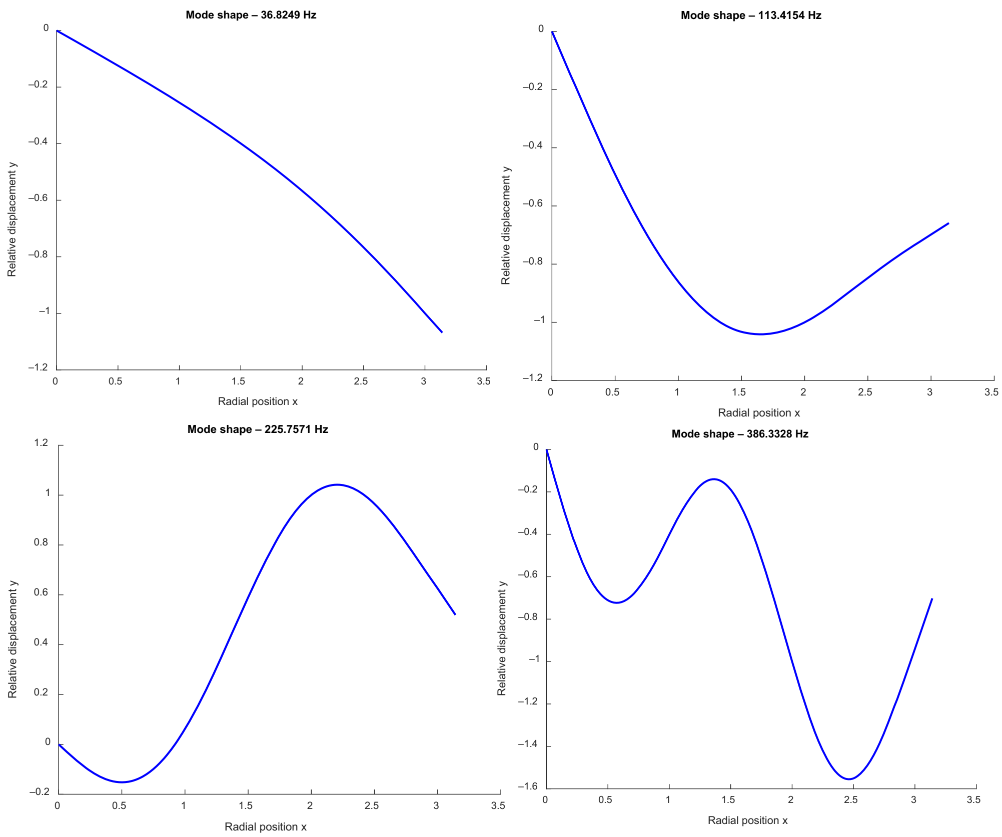

Figure 6 Main rotor blade bending moment function

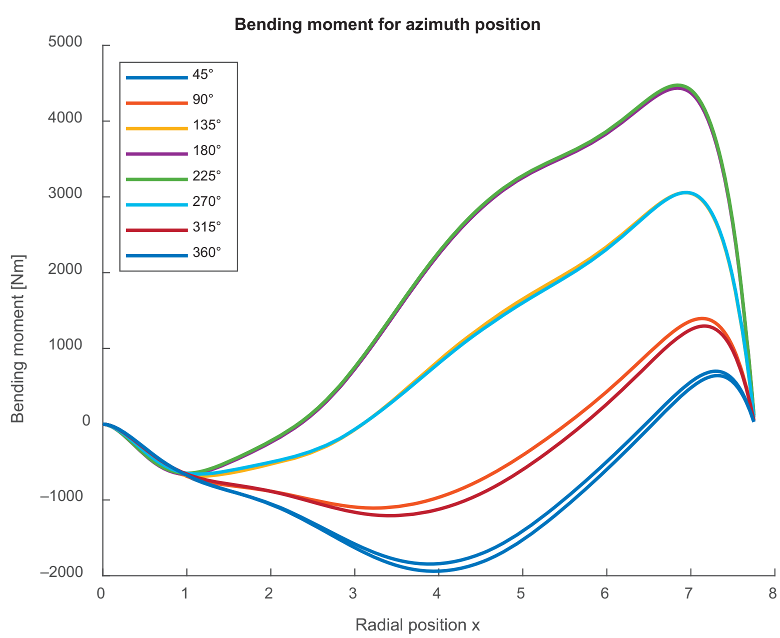

allowing the 3D analysis to provide the total mass of the blade and the mass of the components. The moment acting on a blade in respective sections is loaded from the file generated previously. The strength equations are programmed within the code. Stresses are calculated for each cross section using bending moment values and the moment of inertia from the GRIP analysis. Finally, it is checked whether the required stiffness is sufficient for the given loads. The program adjusts the spar

Figure 7 Main rotor blade CAD model for calculation

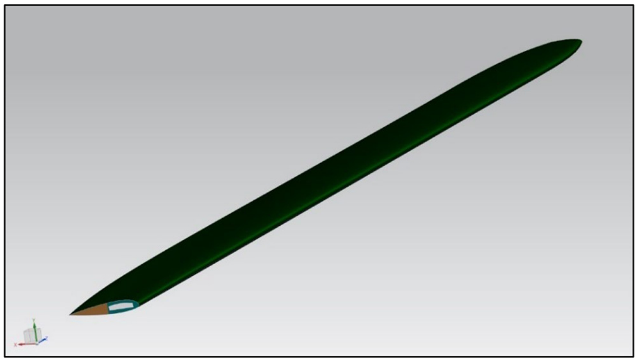

dimensions to meet the stiffness requirement and iterates the calculation until the requirements are met. The iterative procedure modifies the dimensions in each step and evaluates the new shape. A safety factor of 1.2 is proposed, but it can be changed by the user. As a result, a CAD geometry is provided, which can be applied in further complex analysis. An example of the code with analysis options is shown in Figure 8.

Example of results

The steps that were described in the previous chapters were combined into an optimization procedure. The entire procedure is shown in Figure 9.

To demonstrate the capabilities of the procedure, the W-3 helicopter main rotor blade was recalculated using the original blade dimensions and modern materials applied to the proposed structure. The properties of the composite materials used are presented in Table 1.

The procedure was conducted within six iteration loops. The mass reduction and change of the center of mass are shown in Table 2.

In each step, the change of the cross section and consequently the change of the moment of inertia is considered. The geometry is generated automatically, and the output is provided as the blade CAD model. The spar cross section varies along the span in accordance with the calculated bending moments.

Evaluation of the model

To validate the generated model, a one-way FSI simulation is conducted. One-way FSI was chosen to check the optimized structure in simulated blade working conditions. The CFD simulation is proposed as stationary, so the forces produced are transferred one-way to the structure. This approach allows for the assessment of stresses and deformations. In the next research step, a two-way FSI for transient n-blade simulation will be established, taking into consideration the evaluated structure as described in this paper. The CFD part of the simulation is configured for a single-blade fluid enclosure, as demonstrated in the previous part of the research published in Kocjan *et al.* (2022). The pressure distribution from the mentioned CFD simulation is applied to the FEM model. According to MATLAB calculations, the flight conditions for a blade at an azimuthal position of 360° are simulated. The inflow is parameterized using calculated functions. An example of pressure distribution is shown in Figure 10.

Figure 8 Code example

```
SPAR(4)=BSURF/MESH,LNS5(3..4),WITH,LNS3(1..K),TYPE,3,TOLER,.01,.01
SPAR(5)=BSURF/MESH,LNS5(4),LNS5(1),WITH,LNS4(1..K),TYPE,3,TOLER,.01,.01
SPAR(6)=AUTOSF/LNS1(1),LNS2(1),LNS3(1),LNS4(1)
SPAR(7)=AUTOSF/LNS1(K),LNS2(K),LNS3(K),LNS4(K)
SPAR(8)=SEW/SPAR(2..7)

BLD(7)=SEW/SSRF(6..9)
MAT=MATRIX/TRANSL,0,0,0
BLD(5)=TRANSF/MAT,BLD(7)
SPAR(1)=TRANSF/MAT,SPAR(8)

BLD(6)= SUBTRA/BLD(8),WITH,BLD(7),CNT,c $$ enclosure


DELETE/LN,PT2,PT3,PT4,PT5,PT6,SPLC



PLN(1)=PLANE/YZPLAN,C0/3+wall
BLD(1..2)= SPLIT/BLD(5),WITH,PLN(1)

PLN(2)=PLANE/XYPLAN,A(3)+1
SEC(1..3)= SECT/BLD(1),WITH,PLN(2)
BND(1)=BOUND/SEC(1..3)
BND(2)=BOUND/LNS1(1),LNS2(1),LNS3(1),LNS4(1)
ANLSIS/TWOD,BND(1),MMETER,wyn2
ANLSIS/TWOD,BND(2),MMETER,wyn3






PRINT/'--------Spar Cross section analysis-----------'
PRINT/USING,'Cross section area Fdz=#@@@@@@.@@ [mm^2]',wyn2(2)-wyn3(2)
PRINT/USING,'Moment of Intertia Idz=#@@@@@@@.@@ [mm^4]',wyn2(9)-wyn3(9)
PRINT/USING,' center of mass:  X=#@@@@@@@@@@@@.@@@ mm',wyn2(3)
PRINT/USING,'                  Y=#@@@@@@@@@@@@.@@@ mm',wyn2(4)
PRINT/USING,' center of mass:  X=#@@@@@@@@@@@@.@@@ mm',wyn3(3)
PRINT/USING,'                  Y=#@@@@@@@@@@@@.@@@ mm',wyn3(4)
```

Figure 9 Initial structure optimization procedure

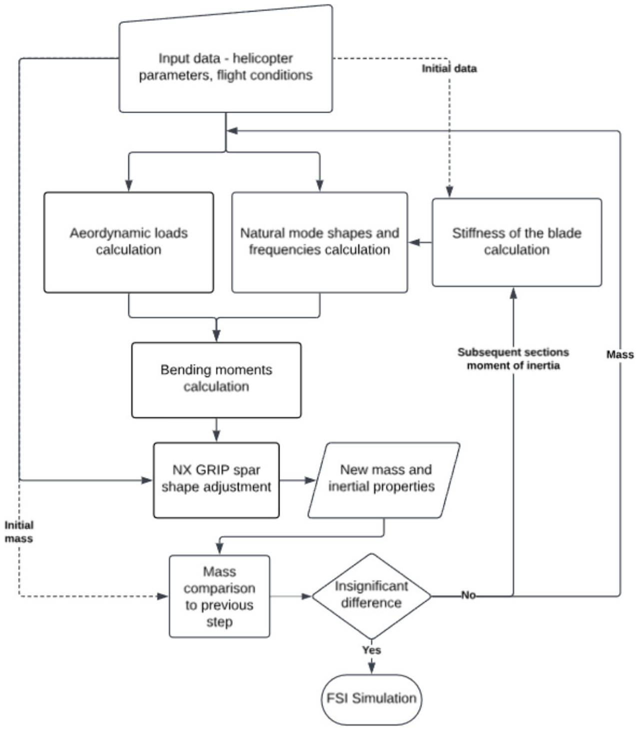

The pressure is transferred to the model generated from the CAD geometry prepared using the algorithm described in this study. The mesh was prepared using the tetrahedral mesher and thin mesher options. The base element size was set at 500 mm, with a target surface size of 0.025 m and a minimum surface size of 0.005 m. The meshing process was fully automated for the imported geometry. The results of the simulation confirm the parameters of the construction and provide information that the model is fully applicable in the FEM analysis environment. Examples of deformation and stresses are shown in Figures 11 and 12.

Discussion

This research introduces a new methodology for preparing geometry for subsequent FEM and FSI analyses. The first section outlines the analytical assumptions for the proposed solution, including calculations for loads and vibrations. The second part provides details on solving analytical problems using modern computer environments, accompanied by a description of the structural optimization method. Furthermore, an example of the resultant geometry with mass effects is presented, along with an evaluation using FSI calculations.

It has been demonstrated that the generated CAD model is fully compatible with FEM software and that meshes can be generated for even extremely complex blade shapes.

The proposed solution offers a novel approach to helicopter design. First, it addresses procedures for resolving natural mode shapes and vibrations of rotating blades, followed by blade trimming under various flight conditions. Furthermore, it provides aerodynamic loading of the blade as a function of radius and azimuth. Finally, the research includes the generation and preparation of a preliminary optimized main rotor blade structural model. These solutions can be used independently or combined for any blade shape and flight conditions.

The results of this research are valuable for reducing the time required to create and evaluate final models for various blade configurations. It is crucial to note that the model has been validated and is ready for implementation in further two-way FSI simulations for full rotor geometry.

To evaluate the solution, the proposed geometry is based on the existing rotor blade shape and dimensions. The forces were calculated using real mission objective parameters (e.g. velocity, height and payload). The flight parameters were also based on data from the Flight Data Recorder. An example of a 1-h flight is shown in Figure 13. The indicated velocity presented in the figure is effective from 50 km/h, due to the stream velocity from the rotor; however, it was not cut out to include the moments when the rotorcraft is on the ground.

Table 2 Iteration results

Step	Mass [kg]	Center of mass [m from rotor axis]
1	60	4.73
2	40.01	4.91
3	35	4.76
4	34.43	4.74
5	34.70	4.79
6	34.70	4.79

Table 1 Material properties

Material property	Gr/E woven cloth	S-glass/E woven cloth	Nomex honeycomb
Young's modulus (E11) [Mpa]	1.69E + 03	6.45E + 02	4.06
Young's modulus (E22) [Mpa]	1.69E + 03	6.26E + 02	4.06
Young's modulus (E33) [Mpa]	2.36E + 02	1.60E + 02	4.06
Shear modulus (G12) [Mpa]	1.32E + 02	1.00E + 02	6.82
Shear modulus (G13) [Mpa]	1.32E + 02	1.00E + 02	6.82
Shear modulus (G23) [Mpa]	1.32E + 02	1.00E + 02	6.82
Poisson ratio (v12)	6.76E − 06	1.65E − 05	4.35E − 05
Poisson ratio (v13)	4.64E − 05	3.92E − 05	4.35E − 05
Poisson ratio (v23)	4.64E − 05	3.92E − 05	4.35E − 05
Density [kg/m^3]	1.60E + 03	1.80E + 03	6.41E + 01

Figure 10 Pressure distribution on the blade

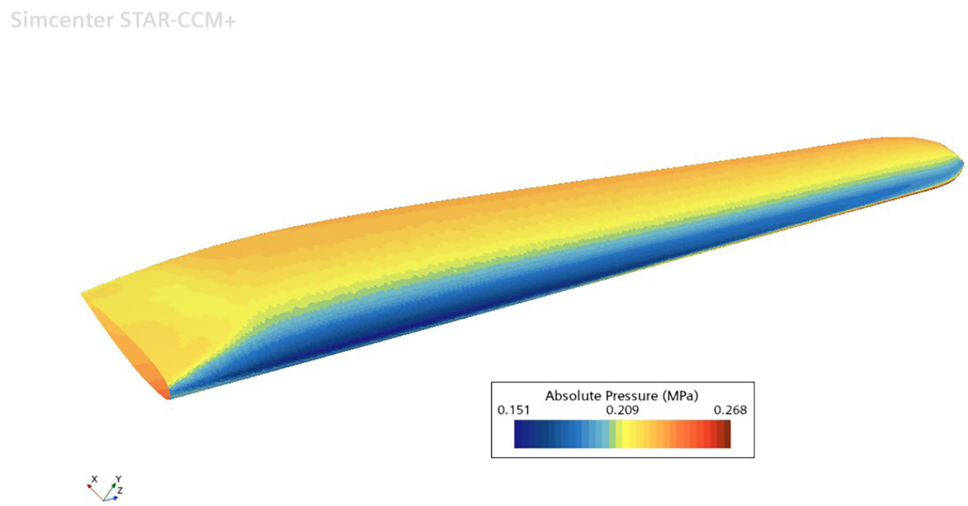

Figure 11 Blade deformation

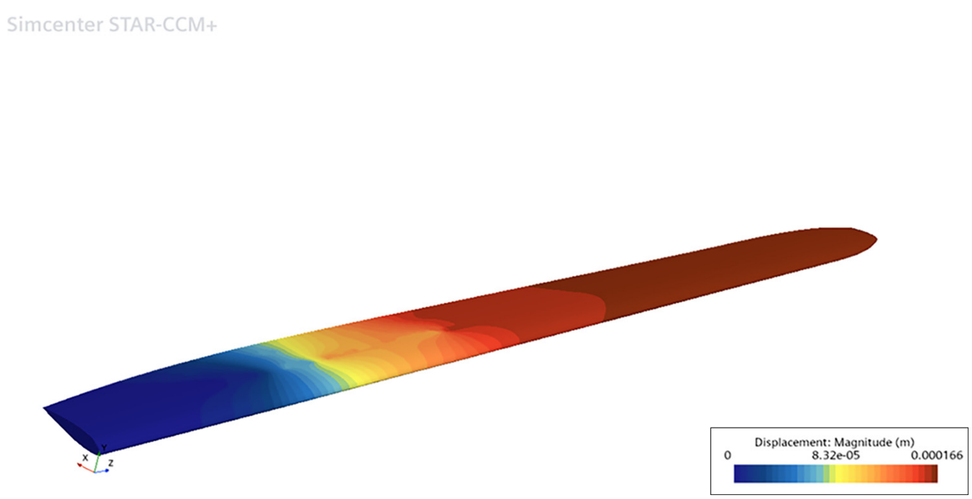

The proposed method is part of wider research; however, the studies described in this paper can be used as a stand-alone procedure during rotorcraft design. The tool can be used to assess the inner structure without integrating it with the proposed rotorcraft optimization procedure. Nevertheless, in this phase, it is limited to the Sikorsky helicopter layout. Nevertheless, the challenge of covering of the various blades structure was achieved for that layout.

Compared to existing design procedures, the main advantage of the presented solution is the versatility of the tool for various blade shapes, materials and environmental conditions, which can be examined in a short time. Practically, it can be implemented in the preliminary design phase of the rotorcraft, allowing many options to be evaluated and some to be chosen for the next design steps. It can also be implemented into the rotor blade lifecycle to assess the existing construction using data acquired during the rotorcraft's life – flight data, maintenance data, airworthiness data, etc.

Conclusion

The initial optimization of the structure is presented in this paper, showcasing a combination of analytical calculations and computer numerical analysis. The optimization of the spar shape was conducted in six steps, with the process lasting approximately 40 min. By parametrizing the spar dimensions in subsequent selected sections, shape optimization was achieved, resulting in the minimum mass of the spar, which has a significantly greater density compared to the remaining elements of the blade.

Considering the potentially time-consuming nature of computer calculations, particularly when simulating an articulated main rotor using FSI, the method outlined in the paper offers an original method to reducing the time required for model preparation for analysis. By inputting desired performance parameters and previously obtained aerodynamic features, the structure can be adapted to fit any proposed blade.

Figure 12 Stress distribution in the blade structure

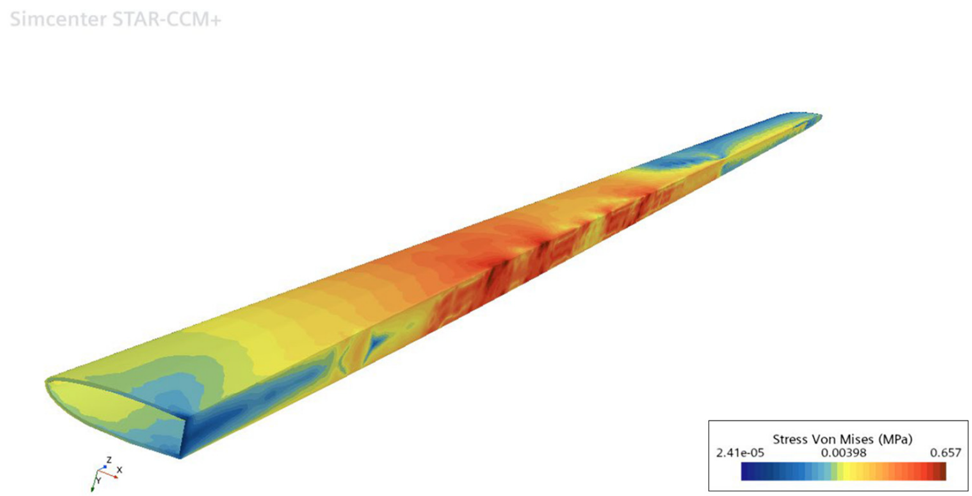

Figure 13 Indicated air speed, barometrical height and g-force

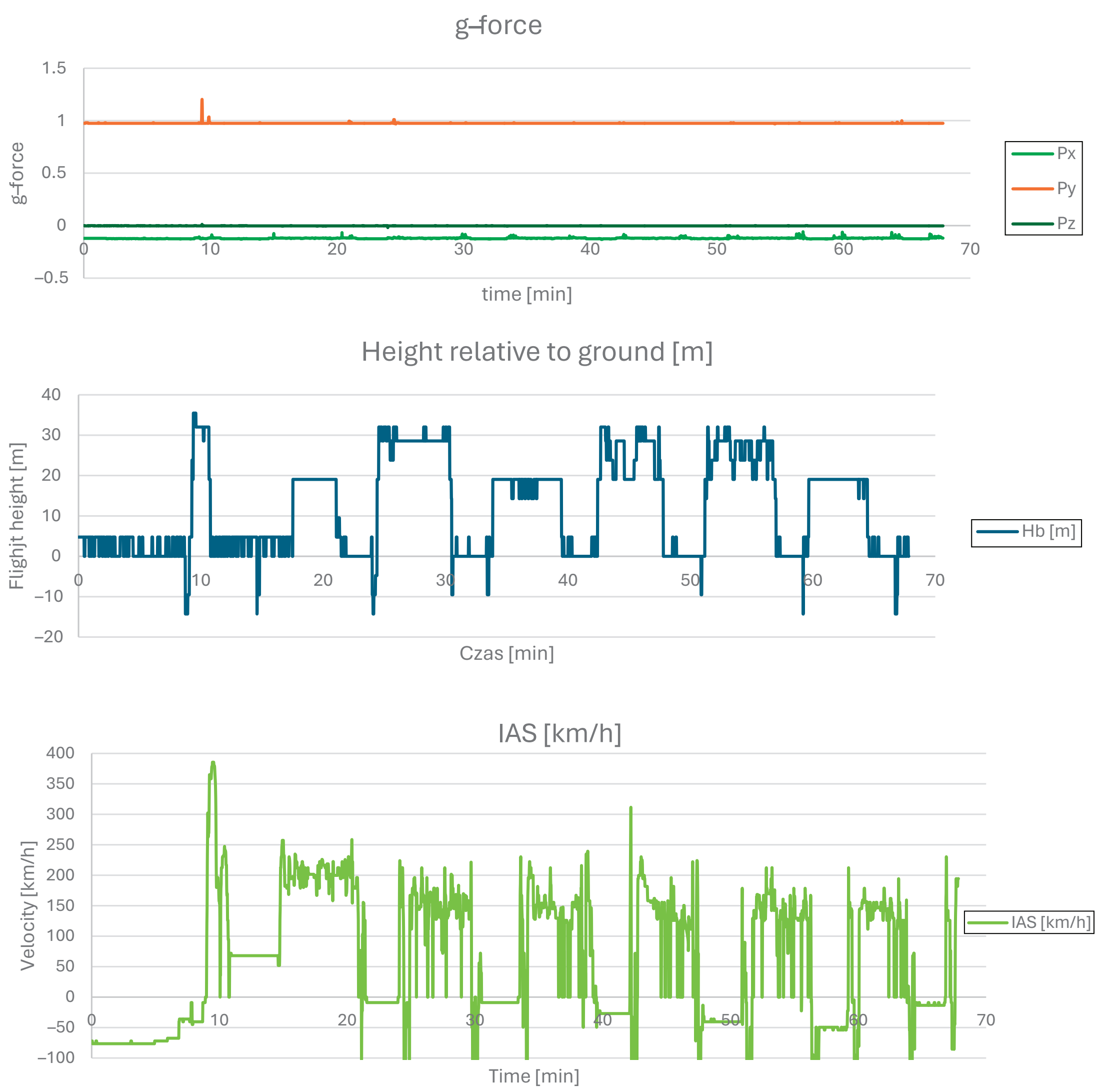

The evaluation of the structure, provided with one-way FSI analysis, demonstrates that the geometry is suitable for CAD/CAE software. Introducing a tool, such as the one presented in this paper, which automates mesh preparation, ensures repeatability of the process for future designs.

In conclusion, the research objectives have been achieved. The preparation method of the model using optimization techniques is ready to be used independently or can be integrated into a comprehensive optimization loop, as intended by the authors for further research endeavors. What is more, even though it is part of a research, the tool is ready to use and can be implemented into the design process as described and used to calculate and assess the blade structure. It can be used in industry to optimize not only the structure but also provide more efficient design and lifecycle analysis.

References

Allen, C.B., Morris, A.M. and Rendall, T.C.S. (2009), "CFD-based aerodynamic shape optimization of hovering rotors", Collection of Technical Papers – *AIAA Applied Aerodynamics Conference*, doi: 10.2514/6.2009-3522.

Allen, L.D., Lim, J.W., Haehnel, R.B. and Dettwiller, I.D. (2021), "Rotor blade design framework for airfoil shape optimization with performance considerations", AIAA Scitech 2021 Forum, doi: 10.2514/6.2021-0068.

Bailly, J., Bailly, D. and Didier, B. (2019), "Multifidelity aerodynamic optimization of a helicopter rotor blade", *AIAA Journal*, Vol. 57 No. 8, pp. 1-13, doi: 10.2514/1.J056513ï.

Barwey, D. and Peters, D.A. (1994), "Optimization of composite rotor blades with advanced structural and aerodynamic modeling", *Mathematical and Computer Modelling*, Vol. 19 Nos 3/4, doi: 10.1016/0895-7177(94)90064-7.

Chattopadhyay, A., McCarthy, T.R. and Pagaldipti, N. (1995), "Multilevel decomposition procedure for efficient design optimization of helicopter rotor blades", *AIAA Journal*, Vol. 33 No. 2, pp. 223-230, doi: 10.2514/3.12424.

Cornette, D., Kerdreux, B., Michon, G. and Gourinat, Y. (2015), "Aeroelastic tailoring of helicopter blades", *ASME. J. Comput. Nonlinear Dynam*, 1 November, Vol. 10 No. 6, p. 061001, doi: 10.1115/1.4027717.

de Guillenchmidt, P. (1951), "Calculation of the bending stresses in helicopter rotor blades", Washington, DC.

Ganguli, R. and Chopra, I. (1996), "Aeroelastic optimization of a helicopter rotor to reduce vibration and dynamic stresses", *Journal of Aircraft*, Vol. 33 No. 4, pp. 808-815, doi: 10.2514/3.47018.

Goerke, D., Le Denmat, A.L., Schmidt, T., Kocian, F. and Nicke, E. (2012), "Aerodynamic and mechanical optimization of CF/PEEK blades of a counter rotating fan", *Proceedings of the ASME Turbo Expo*, Vol. 7, pp. 21-33, doi: 10.1115/GT2012-68797.

Grabowik, C., Kalinowski, K., Kempa, W. and Paprocka, I. (2015), "A method of computer aided design with self-generative models in NX siemens environment", *IOP Conference Series: Materials Science and Engineering*, Vol. 95, p. 012123, doi: 10.1088/1757-899X/95/1/012123.

Guo, J.X. and Xiang, J.W. (2004), "Composite rotor blade design optimization for vibration reduction with aeroelastic constraints", *Chinese Journal of Aeronautics*, Vol. 17 No. 3, pp. 152-158, doi: 10.1016/S1000-9361(11)60230-6.

He, C.J. and Peters, D.A. (1992), "Optimization of rotor blades for combined structural, dynamic, and aerodynamic properties", *Structural Optimization*, Vol. 5 Nos 1/2, pp. 37-44, doi: 10.1007/BF01744694.

Johnson, C., Woodgate, M. and Barakos, G.N. (2016), "Optimising aspects of BERP-like rotors using frequency-domain methods", *Notes on Numerical Fluid Mechanics and Multidisciplinary Design*, Vol. 133, p. 639, doi: 10.1007/978-3-319-27386-0_15.

Kachel, S., Rogólski, R. and Kocjan, J. (2021), "Review of modern helicopter constructions and an outline of rotorcraft design parameters", *Problems of Mechatronics Armament Aviation Safety Engineering*, Vol. 12 No. 3, pp. 27-52, doi: 10.5604/01.3001.0015.2427.

Kizhakke Kodakkattu, S., Nair, P. and Ml, J. (2018), "Design optimization of helicopter rotor using kriging", *Aircraft Engineering and Aerospace Technology*, Vol. 90 No. 6, pp. 937-945, doi: 10.1108/AEAT-12-2016-0250.

Kocjan, J., Kachel, S. and Rogólski, R. (2022), "Helicopter main rotor blade parametric design for a preliminary aerodynamic analysis supported by CFD or panel method", *Materials*, Vol. 15 No. 12, p. 4275, doi: 10.3390/ma15124275.

Lim, J.W. (2018), "Application of parametric airfoil design for rotor performance improvement", 44th European Rotorcraft Forum 2018, ERF 2018, Vol. 1.

Liu, X. and Zhang, B. (2021), "Study on aeroelastic optimal design of composite blades", *Yingyong Lixue Xuebao/Chinese Journal of Applied Mechanics*, Vol. 38 No. 4, doi: 10.11776/cjam.38.04.A011.

Ma, L., Zhao, Q., Zhang, K., Zhang, X. and Zhao, M. (2021), "Aeroelastic analysis and structural parametric design of composite rotor blade", *Chinese Journal of Aeronautics*, Vol. 34 No. 1, pp. 336-349, doi: 10.1016/j.cja.2020.09.055.

Moffatt, S. and Griffiths, N. (2009), "Structural optimisation and aeroelastic tailoring of the BERP IV demonstrator blade", *Annual Forum Proceedings - AHS International*, Vol. 1.

Morris, A.M., Allen, C.B. and Rendall, T.C.S. (2008), "Aerodynamic optimisation of hovering helicopter rotors using efficient and flexible shape parameterisation", Collection of Technical Papers – *AIAA Applied Aerodynamics Conference*, doi: 10.2514/6.2008-7338.

Okumuş, O., Şenipek, M. and Ezertaş, A. (2022), "Multi-objective multi-fidelity aerodynamic optimization of helicopter rotor", AIAA Science and Technology Forum and Exposition, AIAA SciTech Forum 2022, doi: 10.2514/6.2022-2099.

Pahlke, K. and Demaret, B. (2017), "ONERA and DLR contributions to improve environmental friendliness of rotorcraft", *Annual Forum Proceedings - AHS International*.

Ryazanov, A.I. (2016), "Automated 3D modeling of working turbine blades", *Russian Engineering Research*, Vol. 36 No. 9, pp. 751-754, doi: 10.3103/S1068798X16090203.

Sagimbayev, S., Kylyshbek, Y., Batay, S., Zhao, Y., Fok, S. and Lee, T.S. (2021), "3D multidisciplinary automated design optimization toolbox for wind turbine blades", *Processes*, Vol. 9 No. 4, p. 581, doi: 10.3390/pr9040581.

Salh Eddine, D., Smail, K., Mahfoudh, C. and Lyes, T. (2023), "Robust optimization of the aerodynamic design of a helicopter rotor blade based on multi-fidelity meta-models", *Proceedings of the Institution of Mechanical Engineers, Part E: Journal of Process Mechanical Engineering*, Vol. 237 No. 3, pp. 615-634, doi: 10.1177/09544089221111593.

Shabliy, L.S. and Dmitrieva, I.B. (2014), "Conversion of the blade geometrical data from points cloud to the parametric format for optimization problems", *ARPN Journal of Engineering and Applied Sciences*, Vol. 9 No. 10, pp. 1849-1853.

Sinem, M. and Metin Orhan, K.A.Y.A. (2018), "Optimization of vibration reduction in a helicopter blade with 2 way fluid-structure interaction", ASME 2018 Conference on Smart Materials, Adaptive Structures and Intelligent Systems, SMASIS 2018, Vol. 1, doi: 10.1115/SMASIS2018-8017.

Spyropoulos, N., Papadakis, G., Prospathopoulos, J.M. and Riziotis, V.A. (2021), "Investigating the level of fidelity of an actuator line model in predicting loads and deflections of rotating blades under uniform free-stream flow", *Applied Sciences (Switzerland)*, Vol. 11 No. 24, p. 12097, doi: 10.3390/app112412097.

Stalewski, W. (2017), "design and optimisation of main rotor for ultralight helicopter", *Journal of KONES Powertrain and Transport*, Vol. 24 No. 4, p. 24.

Stalewski, W. and Zalewski, W. (2019), "Aerodynamic design and optimisation of main rotors for light rotorcrafts", 45th European Rotorcraft Forum 2019, ERF 2019, Vol. 1.

Straub, F.K., Callahan, C.B. and Culp, J.D. (1992), "Rotor design optimization using a multidisciplinary approach", *Structural Optimization*, Vol. 5 Nos 1/2, pp. 70-75, doi: 10.1007/BF01744698.

Tamer, A., Yücekayali, A. and Ortakaya, Y. (2011), "Design and optimization of helicopter rotor for minimum power required", *6th AIAC Ankara International Aeropsace Conference*, No. September 14-16.

Tarzanin, F., Young, D.K. and Panda, B. (1999), "Advanced aeroelastic optimization applied to an improved performance, low vibration rotor", *Annual Forum Proceedings – American Helicopter Society*, Vol. 1, pp. 183-194.

Tian, S., Tao, F., Du, H., Yu, W., Lim, J.W., Haehnel, R., Wenren, Y., *et al* (2022),. "Structural design optimization of composite rotor blades with strength considerations", AIAA Science and Technology Forum and Exposition, AIAA SciTech Forum 2022, doi: 10.2514/6.2022-2454.

Tixadou, E. (2021), "optimisation of the structure of a helicopter blade in view of reducing cabin vibration".

Tremolet, A. and Basset, P.M. (2012), "Some meta-modeling and optimization techniques for helicopter pre-sizing", 38th European Rotorcraft Forum 2012, ERF 2012, Vol. 2.

Vu, N.A. and Lee, J.W. (2015), "Aerodynamic design optimization of helicopter rotor blades including airfoil shape for forward flight", *Aerospace Science and Technology*, Vol. 42, pp. 106-117, doi: 10.1016/j.ast.2014.10.020.

Vu, N.A., Lee, J.W., Le, T.P.N. and Nguyen, S.T.T. (2016), "A fully automated framework for helicopter rotor blades design and analysis including aerodynamics, structure, and manufacturing", *Chinese Journal of Aeronautics*, Vol. 29 No. 6, pp. 1602-1617, doi: 10.1016/j.cja.2016.10.001.

Wang, H., Zhang, B. and Li, D. (2013), "The research on helicopter rotor aeroelastic dynamics multi-objective optimization solution", Vol. 30, pp. 217-222, doi: 10.11776/cjam.30.02.B103.

Wilde, E. and Price, H.L. (1965), "A theoretical method for calculating flexure and stresses in helicopter rotor blades", *Aircraft Engineering and Aerospace Technology*, Vol. 37 No. 2, pp. 45-54.

Wilke, G. (2021), "Quieter and greener rotorcraft: concurrent aerodynamic and acoustic optimization", *CEAS Aeronautical Journal*, Vol. 12 No. 3, pp. 495-508, doi: 10.1007/s13272-021-00513-x.

Wilke, G. (2024), "Jaxa-onera-dlr cooperation: results from rotor optimization in hover".

Xie, J., Xie, Z., Zhou, M. and Qiu, J. (2017), "Multidisciplinary aerodynamic design of a rotor blade for an optimum rotor speed helicopter", *Applied Sciences (Switzerland)*, Vol. 7 No. 6, p. 639, doi: 10.3390/app7060639.

Гребеников, АГ., Дьяченко, ЮВ., Коллеров, ВВ., Коцюба, ВЮ., Малков, ИВ., Урбанович, ВА. and Воронько, ИА. (2021), "Analysis of design and technological features of the main rotor blades of heavy transport helicopters", *Open Information and Computer Integrated Technologies*, Vol. 93, pp. 59-103, doi: 10.32620/oikit.2021.93.04.

Further reading

Johnson, W. (1994), *Helicopter Theory, Dover Publications, INC*, Dover Publications, New York, NY.

Rotaru, C., Cîrciu, I. and Luculescu, D. (2016), "Lift capability prediction for helicopter rotor blade-numerical evaluation", *AIP Conference Proceedings*, Vol. 1738, doi: 10.1063/1.4952208.

Corresponding author

Jakub Kocjan can be contacted at: jakub.kocjan@wat.edu.pl